Available online at www.sciencedirect.com
SCIENCE DIRECT®
Polymer 46 (2005) 6226–6234
polymer
www.elsevier.com/locate/polymer

Understanding multivinyl monomer photopolymerization kinetics through modeling and GPC investigation of degradable networks

Tara M. Lovestead[a], Jason A. Burdick[a,1], Kristi S. Anseth[a,b], Christopher N. Bowman[a,c,*]

[a]Department of Chemical and Biological Engineering, University of Colorado, Boulder, CO 80309-0424, USA
[b]Howard Hughes Medical Institute, University of Colorado, Boulder, CO 80309-0424, USA
[c]Department of Restorative Dentistry, University of Colorado Health Sciences Center, Denver, CO 80045-0508, USA

Received 12 November 2004; received in revised form 10 March 2005; accepted 11 March 2005
Available online 13 June 2005

Abstract

Multivinyl monomers that react to form highly crosslinked, biodegradable networks are being developed as scaffolds for tissue engineering and vehicles for drug delivery; however, this work demonstrates their usefulness in characterizing better the complexities of the kinetics and structural evolution during crosslinking photopolymerization. The molecular weight distributions (MWDs) of the degradation products of networks formed through the free radical photopolymerization of multivinyl monomers validate a novel kinetic model to test hypotheses as to the important kinetic mechanisms during crosslinking. The kinetic model, in conjunction with the experimental results for the degradable network, provides insight into the fundamental termination mechanisms (i.e. chain length dependent termination (CLDT), chain transfer to either a unimolecular species or polymer, and the accumulation of persistent radicals) that control the MWD of the backbone kinetic chains throughout the polymerization. Specifically, the importance of CLDT during autoacceleration and the impact of light intensity on the MWD of the backbone kinetic chains are presented.

Keywords: Crosslinking; Kinetic chains; Photopolymerization

1. Introduction

Multivinyl monomers photopolymerize to produce highly crosslinked networks with exceptional material properties. Photopolymerization occurs when an ultraviolet (UV) or visible light absorbing species cleaves into initiating radicals that propagate through the monomer's vinyl groups. If the monomer contains multiple vinyl groups, a crosslinked network forms, which affords increased strength, toughness, and chemical resistance over linear polymers. The photopolymerization reaction occurs under ambient conditions, does not require a solvent, is rapid when compared to thermal polymerizations, and provides spatial and temporal control. Additionally, flexible monomer chemistry and functionality allow control over the resulting polymer network's biocompatibility, crosslinking density, and mechanical strength. For these numerous reasons, photopolymer networks are attractive industrially and are currently used for a variety of applications, including microelectronics, contact lenses, dental restorations, adhesives, and coatings and are being extensively researched in the biomaterials field [1–8].

Despite the numerous applications for multivinyl monomer photopolymerizations, a complete understanding of the kinetics and structural evolution is lacking. Our lack of fundamental understanding of these systems is due, in part, to the insoluble, crosslinked network that forms, which renders analysis of the molecular weight distribution (MWD) of the backbone kinetic chains difficult [9–12]. One method to overcome this difficulty is the selection of monomers with degradable linkages. For example, methacrylated sebacic acid (MSA, Fig. 1) forms a highly crosslinked, biodegradable polymer network that, upon hydrolysis of labile anhydride linkages, degrades exclusively into sebacic acid and poly(methacrylic acid) kinetic chains [13–16]. Thus, the MWD of the degradation products can be isolated and characterized, providing insight into

---

* Corresponding author. Tel.: +1 303 492 3247; fax: +1 303 492 4341.
E-mail address: christopher.bowman@colorado.edu (C.N. Bowman).

[1] Present address: Department of Chemical Engineering, Massachusetts Institute of Technology, Cambridge, MA 02139, USA.

0032-3861/$ - see front matter © 2005 Elsevier Ltd. All rights reserved.
doi:10.1016/j.polymer.2005.03.112

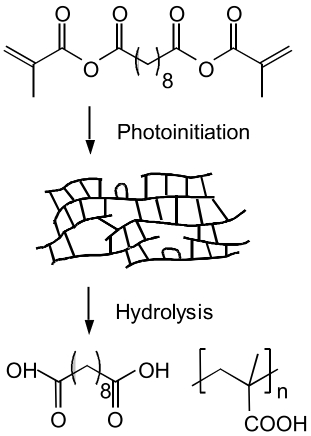

Fig. 1. Chemical structure of methacrylated sebacic acid (MSA), which forms a highly crosslinked network via a photoinitiated chain polymerization and degrades upon hydrolysis of the labile anhydride linkages in the crosslinks into sebacic acid and poly(methacrylic acid) kinetic chains.

multivinyl monomer photopolymerization kinetics and network formation.

Anseth and co-workers explored experimental techniques, both matrix assisted laser desorption/ionization time-of-flight mass spectrometry and gel permeation chromatography (GPC), to investigate the effect of the initiation rate on MSA's post-degradation molecular weight distribution [15,17]. These experiments provide further insight into how changing initiation conditions impact the kinetic chain lengths post-degradation for highly crosslinked networks. Both studies revealed that when MSA is polymerized with an increased light intensity that the cumulative MWD of the degradation products is comprised of shorter kinetic chains, i.e. shorter average kinetic chain lengths are released upon degradation of the crosslinks. Additionally, the degradation product's MWDs were observed to shift towards longer, and then shorter, kinetic chain lengths during autoacceleration and autodeceleration, respectively. Autoacceleration is the counterintuitive increase in the polymerization rate as the growing radical chains becomes mobility restricted, and autodeceleration is the rapid decrease in the polymerization rate once the small monomer molecule becomes mobility restricted, i.e. diffusion controlled termination and propagation, respectively. These regimes are represented in Fig. 2, which presents the model's prediction of the polymerization rate versus double bond conversion for a typical multivinyl monomer photopolymerization.

The experimental results of Anseth and co-workers provide useful information as to how polymerization time, reacting system mobility, and initiation rate impact the MWD of the degradation products. Fundamental understanding of multivinyl monomer photopolymerization kinetics and network evolution is improved further when kinetic models are used to test hypotheses related to the important mechanism(s) that control the degradation product's MWD. The termination mechanism is the most complex and least understood aspect of photopolymerization kinetics, and thus, modeling efforts are focused on exploring the impact of different termination mechanisms on structural evolution. By combining model predictions with previously reported experimental results, insight as to how different termination mechanisms impact the characteristics of the MWD of the degradation products is obtained. Ultimately, an enhanced fundamental understanding of multivinyl monomer photopolymerization kinetics and network formation enables the tailoring and optimization of polymer network attributes by changing monomer chemistry and photopolymerization conditions.

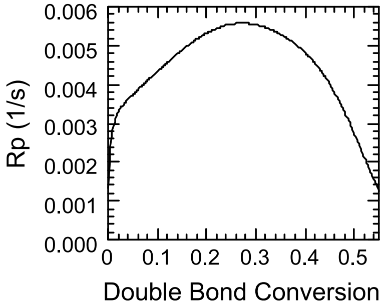

Fig. 2. The polymerization rate as a function of double bond conversion is presented for a typical multivinyl monomer photopolymerization that exhibits autoacceleration leading to a maximum polymerization rate, followed by autodeceleration.

2. Model development

Several authors have utilized mathematical models to investigate MWDs in monovinyl free radical polymerizations to include branching via chain transfer and/or termination by disproportionation [18–22], crosslinking reactions both with [23,24] and without chain length dependent termination (CLDT) [25], and pulsed laser polymerizations that take into account chain transfer to monomer and intramolecular chain transfer to polymer (cyclization) [26,27]. The model presented herein differs from previous models in that the model accounts for diffusion control of the kinetic constants, predicting typical multivinyl monomer photopolymerization phenomena, such as, autoacceleration [11,28–36], reaction diffusion controlled termination [37–42], autodeceleration, and incomplete double bond conversion when the cure temperature is below the polymer's glass transition temperature (T_g) [43–45]. CLDT is also accounted for, enabling more accurate prediction of the initiation rate's impact on the photopolymerization kinetics. Additionally, the model does not use the pseudo steady state assumption on the radical concentrations and does not differentiate between radicals incorporated in the gel versus the sol; therefore, the model predicts the MWD as if all of the crosslinks were broken to release the kinetic chains.

Multivinyl monomer photopolymerization is extremely difficult to model due to the rapid generation of high molecular weight and crosslinked polymer, which increases the reacting system's viscosity and induces complex diffusion restrictions on the reacting species [11,46,47]. Model development begins by incorporating the most important photopolymerization reactions: initiation, propagation, and termination [48,49]. Although classical kinetics does not apply to the majority of multivinyl monomer polymerizations, the classical assumptions provide a foundation for developing more complex models. Classical kinetics assumes chain length independent bimolecular termination and pseudo-steady state radical concentrations, predicting that the polymerization rate (R_p) depends on the initiation rate (R_i) to the 1/2 power (Eq. (1), where α is the scaling exponent that describes this relationship) [48,49].

$$R_p = \frac{k_p}{\sqrt{2k_t}}[\mathrm{C}=\mathrm{C}]R_i^{\alpha} \tag{1}$$

Here, k_p and k_t are the propagation and termination kinetic constants, respectively, and [C=C] is the double bond concentration. One way to obtain information about the termination mechanism is to photopolymerize several samples at different initiation rates and measure the impact of changing the initiation rate on the polymerization rate, i.e. α. If the termination mechanism deviates from classical kinetics, and this deviation is quantifiable, then α will deviate from the classical 1/2 value. Non-classical termination is observed often and has been attributed generally to the complex diffusion limitations (autoacceleration, autodeceleration, reaction diffusion controlled termination, and persistent radical accumulation, i.e. radical trapping on the time-scale of the polymerization reaction) that arise during network formation.

In monovinyl systems, it is well documented that increasing viscosity of the reacting system and diffusion control of the growing radical chains result in CLDT [35,44,50–57]. When chain length dependent termination is important, short radical chains are more mobile, and thus, terminate more readily than less mobile, long radical chains. One way to evaluate the importance of CLDT during photopolymerization is to evaluate the impact of the cure condition on the polymerization kinetics. When CLDT is relevant, any cure condition that impacts the average kinetic chain length of the radical chains will impact the termination rate, and thus, the polymerization kinetics [44,54,57,58]. For example, if increasing the initiation rate shifts the molecular weight distribution of the growing radical chains towards a shorter average kinetic chain length, then the termination rate will increase due to more facile termination.

While CLDT is counterintuitive in multivinyl monomer polymerizations due to the rapid formation of a highly crosslinked network, or gel, recent researchers have demonstrated the importance of chain length dependencies during the photopolymerization of both poly(ethylene glycol)-600 dimethacrylate, (PEG600DMA) and di(ethylene glycol) dimethacrylate (DEGDMA) [37,59,60]. These are interesting monomers to investigate because they both differ significantly in their glass transition temperature, resulting in the formation of a rubbery versus a glassy polymer network when PEG600DMA and DEGDMA, respectively, are photopolymerized. The experimental observation of a less than expected increase in the polymerization rate when the initiation rate was increased, i.e. CLDT, in both monomer systems is remarkable due to the very different network structures that are formed. To gain insight into the CLDT experimentally observed during multivinyl monomer photopolymerization, a kinetic model that incorporates chain length dependencies into the mathematical equations that describe termination in these systems was developed [37,61].

This kinetic model is based on previous models of crosslinking phenomena that account for the effects of increasing polymer concentration on the reacting species mobility and diffusivity via the mathematical expressions for k_p and k_t [43,62–65]. Reaction diffusion controlled termination is modeled according to the theory developed by Anseth and Bowman [64]. A complete kinetic model description is presented in Lovestead et al. [61]. In brief, Allen and Patrick [44] and Benson and North [50] were two of the first groups to propose a relationship for the termination event's dependence on the initiation rate. The CLDT theory of Benson and North is incorporated as a one-parameter correction to the termination kinetic constant for two unimer radicals, $k_{t0}^{1,1}$, in the mass transfer limited regime, where $k_{t0}^{i,j}$ is a function of the chain length (i or j) of the two terminating radical chains.

$$k_{t0}^{i,j} = k_{t0}^{1,1}\frac{1}{2}\left(\frac{1}{i^{\gamma}}+\frac{1}{j^{\gamma}}\right) \tag{2}$$

Here, γ describes the extent that increasing the radical chain length decreases the radical's ability to terminate. Coupling this expression to those that have been developed to account for diffusion controlled kinetics, free volume considerations, and reaction diffusion controlled termination yields the desired CLDT kinetic constant ($k_t^{i,j}$) [37,61,66].

$$k_t^{i,j} = k_{t0}^{1,1}\left\{1+\left(\frac{1}{2}\left(\frac{1}{i^{\gamma}}+\frac{1}{j^{\gamma}}\right)\exp\left(-A_t\left(\frac{1}{f}-\frac{1}{f_{ct}}\right)\right)\right.\right.$$
$$\left.\left.+\frac{Rk_p[\mathrm{C}=\mathrm{C}]}{k_{t0}^{1,1}}\right)^{-1}\right\}^{-1} \tag{3}$$

Eq. (3) describes how the termination kinetic constant for two radical chains of arbitrary length i or j depends on the fractional free volume of the system, and thus, the double bond conversion. A more detailed discussion of fractional free volume dependent kinetics appears in Lovestead et al. [61]. In brief, as the extent of conversion increases the termination mechanism transitions from mass transfer control to reaction diffusion controlled termination. In this expression, A_t is a constant that controls the onset and rate of autoacceleration; f_{ct} is the critical fractional free volume where termination becomes controlled by the diffusion of the radical chains or chain ends; and f is the fractional free volume of the system [43,64,65,67]. Additionally, R is the reaction diffusion parameter, or the ratio of kinetic constants, $k_t/(k_p[\mathrm{C{=}C}])$, when reaction diffusion is the dominant termination mechanism [64].

CLDT is thought to occur predominantly at low double bond conversion when the network is more dilute and short, unattached radical chains are still able to diffuse (Fig. 3(a)). As the network continues to form and most of the radicals become tethered to the network, and termination occurs predominantly by reaction diffusion controlled termination, a chain-length independent mechanism (Fig. 3(b)). Eq. (3) reflects gel formation as increasing double bond conversion induces a transition from CLDT to reaction diffusion controlled termination.

Radical concentrations of each length are accounted for, thus, information about the concentrations of the 'living' radical chains and the 'dead' kinetic chains is provided. The MWD represents the weighted contribution of both the 'living' and 'dead' kinetic chains, though the living fraction is typically very small. For simplicity, all polymeric radicals are assumed to terminate via disproportionation. This assumption is appropriate for most methacrylate monomer systems [48]. Additionally, each radical chain length is accounted for, therefore, the polymerization rate is calculated exactly, without using the pseudo-steady state assumption on the radical concentrations [37,61,66].

$$R_p = -\frac{\mathrm{d}[\mathrm{C}=\mathrm{C}]}{\mathrm{d}t} = k_p[\mathrm{C}=\mathrm{C}][\mathrm{P}^{\cdot}]_{\mathrm{tot}} \qquad (4)$$

Here, $[\mathrm{P}^{\cdot}]_{\mathrm{tot}}$ is the total radical concentration and t is the polymerization time.

For a truly 'exact' solution, an infinite number of radical specie's balances is required. These balances are made more tractable by well justified assumptions of averaging together longer length radicals and assuming groups of radicals that are similar in chain length are equally reactive [57,61]. The chain length independent propagation kinetic constant, k_p, initiation rate, initiator decay, and chain transfer to both a unimolecular species and polymer are incorporated as appear in previous manuscripts [61,66]. Additionally, the model includes expressions for the accumulation of persistent radicals. As a crosslinked network forms, persistent polymeric radicals 'trap' on the time-scale of the polymerization reaction. Persistent radical accumulation is modeled to increase with increasing polymer formation according to Eq. (5) [68].

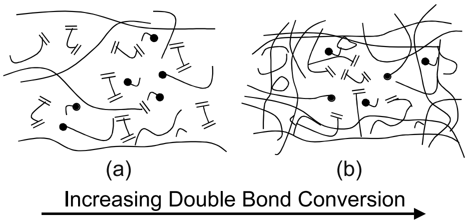

Fig. 3. A schematic of a typical multivinyl monomer photopolymerization at both low (a) and high double bond conversion (b) is presented.

$$\frac{\mathrm{d}[\mathrm{P}_i^{\cdot}]_{\mathrm{trap}}}{\mathrm{d}t} = k^*[\mathrm{P}^{\cdot}]_{\mathrm{tot}} \qquad (5)$$

$$k^* = k_{\mathrm{UMT}}\exp\left(\frac{A_{\mathrm{trap}}}{f}\right) \qquad (6)$$

Here, $[\mathrm{P}_i^{\cdot}]_{\mathrm{trap}}$ is the persistent radical concentration, k^* is the termination kinetic constant that describes persistent radical accumulation; k_{UMT} is the unimolecular termination (UMT) kinetic constant at infinite fractional free volume, and A_{trap} is a constant that controls the rate and onset of persistent radical accumulation.

3. Model parameters

The model is a useful tool for testing hypotheses about the important mechanism(s) during multivinyl monomer photopolymerization that impact the kinetics and network evolution. Di(ethylene glycol) dimethacrylate (DEGDMA) is a good monomer system to model because it exhibits chain length dependent termination, autoacceleration, reaction diffusion controlled termination, and incomplete double bond conversion. Additionally, DEGDMA is similar in monomer chemistry and functionality to MSA, the monomer system investigated experimentally, which is used to validate the model and gain insight into the important termination mechanisms during photopolymerization and structural evolution. DEGDMA's material properties ($T_{g,m} = -12$ °C [69], $T_{g,p} = 500$ °C [69], $\rho_m = 1.06$ g/cm^3 [63,64,69], and $\rho_p = 1.32$ g/cm^3 [63,64,69]), where m and p represent monomer and polymer, respectively, and ρ is density, are taken from the literature. The reaction diffusion coefficient ($R = 2000$ cm^3/mol) was characterized by both Anseth et al. and Berchtold et al. [60,70].

The model parameters for the diffusion control and free volume effects on termination and propagation, along with CLDT, ($k_{p0} = 0.05$ m^3/(mol s), $k_{t0}^{1,1} = 90$ m^3/(mol s), $A_p = 0.18$, $A_t = 0.43$, $f_{cp} = 0.02$, $f_{ct} = 0.037$, and $\gamma = 0.8$) predict the aforementioned complex photopolymerization phenomena observed during DEGDMA photopolymerization. The chain length independent model parameters predict the equivalent polymerization rate behavior as the CLDT model at 2.5 mW/cm^2 with 0.1 wt% photoinitiator ($k_{p0} = 0.05$ m^3/(mol s), $k_{t0}^{1,1} = 11$ m^3/(mol s), $A_p = 0.18$, $A_t = 0.52$, $f_{cp} = 0.02$, $f_{ct} = 0.045$, and $\gamma = 0.0$). Additionally, the parameters for the photoinitiator, 2,2-dimethoxy-2-phenyl acetophenone (DMPA), a common ultraviolet initiator, along with the initiator decay rate and the parameters for 1-dodecanthiol, a typical chain transfer agent, appear in a previous manuscript [61]. The parameter values ([CT] = 0.5 M, $k_{CTP} = 2000$ cm^3/(mol s), $k_{trap} = 0.1$ cm^3/(mol s), $A_{trap} = 0.25$, where [CT] is the chain transfer agent concentration; k_{CTP} and k_{trap} are the kinetic constants for chain transfer to polymer and persistent radical accumulation, respectively; and A_{trap} describes the rate and onset of persistent radical accumulation) are selected to predict trends of increasing chain transfer and persistent radical accumulation with increasing double bond conversion [68].

4. Experimental design

4.1. Network synthesis and degradation

Dimethacrylated sebacic acid (MSA, Fig. 1) was synthesized as described in detail elsewhere [16]. All materials were used as received from Aldrich unless noted otherwise. DMPA (Ciba-Geigy) at a concentration of 0.1 wt% was dissolved in MSA at ~60 °C. Samples were polymerized at room temperature between glass slides with a spacing of 0.5 mm using a Novacure (XFOS) light source with a 365 nm filter at either 2.5 or 25.0 mW/cm^2 for 5 min. Samples were degraded completely in 0.5 M NaOH, neutralized with 1 M HCl, transferred to cellulose ester dialysis tubing (Spectra/Por, Spectrum Laboratories) with a 500 Da molecular weight cut off, dialyzed to remove salts, frozen at −80 °C, and lyophilized for storage before GPC analysis. All sample conditions were performed at least in duplicate.

4.2. Reaction characterization

The photopolymerization behavior of MSA with polymerization time was characterized using differential scanning calorimetry (DSC, Perkin–Elmer DSC7). Isothermal conditions were maintained at room temperature with an external chiller (NESLAB RTE-111) attached to the DSC. The MSA/initiator sample (~5 mg) was placed in the bottom of an aluminum DSC pan, and the heat flux was monitored during irradiation as described above. The polymerization rate was obtained using a ΔH_{rxn} of −55,000 kJ/mol [71], and the double bond conversion was obtained by integrating the polymerization rate versus time curve.

4.3. GPC analysis of kinetic chains

Lyophilized samples were dissolved in 0.1 M $NaNO_3$ buffer, and filtered through a 0.45 μm syringe filter before manual injection into a GPC system (Waters 515 HPLC pump, 1 mL/min, 35 °C) equipped with Polymer Standard Services Suprema Columns (Guard, Linear, 30, 100, 1000 Å) and a Waters refractive index detector (Model 2410). The molecular weights and polydispersity of the degradation products were calibrated using poly (methacrylic acid) (PMAA) molecular weight standards (polymethacrylic acid sodium salt, $M_p = 1000$–1,000,000, Polymer Standards Service, USA, where M_p is the molecular weight at the peak maximum).

5. Results and discussion

The complex termination kinetics associated with diffusion control, coupled with the formation of a highly crosslinked network, makes characterization and analysis of multivinyl monomer photopolymerization difficult. MSA, a monomer system that photopolymerizes to form a highly crosslinked network and yet has degradable crosslinks, is useful to obtain the MWD of the kinetic chains and affords insight into the effects of initiation rate on structural evolution [15,17]. Here, an experimental result for MSA's backbone MWDs that result from hydrolytic cleavage of crosslinks in what, before degradation and during polymerization, was a highly crosslinked polymer is used to guide model investigation of network formation.

Poly(MSA)'s backbone molecular weight evolution with double bond conversion is presented in Table 1. Briefly, the cumulative number average kinetic chain length ($\bar{n}_i$) increases and then decreases with double bond conversion, accompanied by a decrease in the cumulative kinetic chain length polydispersity (Q). Examining the MWD of the backbone kinetic chains from MSA's photopolymerization and, subsequently, degradation provides insight into crosslinking kinetics and network formation. These prior experimental observations provide a basis for focusing modeling efforts to evaluate hypotheses as to which kinetic mechanisms impact the MWD of the backbone kinetic chains. The kinetic model probes the impact of CLDT, chain transfer to both a unimolecular species and polymer, and persistent radical accumulation on the MWD in the regions that typify photopolymerization kinetics, i.e. autoacceleration and autodeceleration. The versatility of the kinetic model enables a greater fundamental understanding of the complex termination mechanism. The remainder of this manuscript presents model predictions aimed at obtaining a

Table 1
The cumulative number average kinetic chain length ($\bar{n}_i$) and the degradation product's cumulative polydispersity (Q) during the polymerization of MSA are presented

Conversion (%)	$\bar{n}_i$	Q
4	1600	2.8
30	2200	2.6
60	2000	1.7

All polymerizations are with 0.1 wt% DMPA at 2.5 mW/cm^2 ultraviolet light. The polymerization rate was monitored with DSC, and double bond conversion was determined by integrating the polymerization rate versus time curve. Double bond conversions reflect values at the onset of autoacceleration (4%), around the maximum R_p (30%), and during autodeceleration (60%). Experimental data from Burdick and co-workers [15].

Table 2
The CLDT model predictions of the cumulative number average kinetic chain length ($\bar{n}_i$) and the backbone kinetic chains' cumulative polydispersity (Q) for a typical multivinyl monomer photopolymerization with 0.1 wt% DMPA at 2.5 mW/cm^2 ultraviolet light are presented

Conversion (%)	$\bar{n}_i$	Q
15	1590	2.5
30	1950	2.4
45	2110	2.3
50	2070	2.3

Double bond conversions reflect values at the onset of autoacceleration (15%), around the maximum R_p (30%), during autodeceleration (45%), and when the polymerization rate is near zero (50%).

better understanding of network formation during multivinyl monomer photopolymerization.

The model with and without accounting for CLDT (Tables 2 and 3, respectively) reveals that the cumulative number average kinetic chain length increases and decreases throughout autoacceleration and autodeceleration, respectively (i.e. from 15 to 30 and from 30 to 45% double bond conversion, respectively), and is independent of CLDT. In spite of this agreement, the cumulative kinetic chain length polydispersity is impacted by CLDT. While the CLDT model predicts that Q decreases throughout autoacceleration, i.e. prior to 30% double bond conversion, the non-CLDT model predicts that Q is constant throughout autoacceleration. Both the CLDT and the non-CLDT models predict that Q decreases throughout autodeceleration, i.e. from 30 to 45% double bond conversion (Tables 2 and 3). CLDT dictates that short radical chain termination is more facile and that long radical chain termination is retarded, when comparing to the average termination rate. Thus, a system that exhibits CLDT will yield a broader MWD with a higher cumulative kinetic chain length polydispersity (Fig. 4). Since, typically, free radical chain photopolymerizations generate heterogeneous chain length distributions, the remainder of this manuscript presents the model that accounts for chain length dependent termination.

A deeper understanding of network formation is also obtained by examining the cumulative kinetic chain length polydispersity throughout the entire photopolymerization. Interestingly, the CLDT model predicts that Q increases until ~10% double bond conversion (Fig. 5). More insight is also obtained by investigating the impact of chain transfer reactions on the structural evolution. When chain transfer to a unimolecular species (CTM) is the dominant chain breaking mechanism, the model predicts a more 'classical' photopolymerization where the polydispersity is relatively constant until autodeceleration (Fig. 5). Significant CTM also generates a narrower MWD of the backbone kinetic chains (Fig. 6(b)). The increase in the cumulative kinetic chain length polydispersity during autodeceleration is due to continued growth of the long chain radicals concomitant with the continued generation of short chain radicals via chain transfer. Additionally, under these circumstances, the model predicts that significant chain transfer to polymer (CTP) increases Q throughout the polymerization (Fig. 5). This increase in Q is due to chain transfer preferentially occurring with higher molecular weight polymer. Thus, the longer kinetic chains grow even longer, while the short radical chains remain short, resulting in a broader MWD of the backbone kinetic chains (Fig. 6(a)). As more polymer is formed the short and long radical chain peaks shift towards even shorter and longer, respectively, average molecular weights.

Table 3
The non-CLDT model predictions of the cumulative number average kinetic chain length $\bar{n}_i$ and the backbone kinetic chains' cumulative polydispersity (Q) for a typical multivinyl monomer photopolymerization with 0.1 wt% DMPA at 2.5 mW/cm^2 ultraviolet light are presented

Conversion (%)	$\bar{n}_i$	Q
15	1580	2.0
30	1950	2.0
45	2110	2.1
50	2080	2.1

Double bond conversions reflect values at the onset of autoacceleration (15%), around the maximum R_p (30%), during autodeceleration (45%), and when the polymerization rate is near zero (50%).

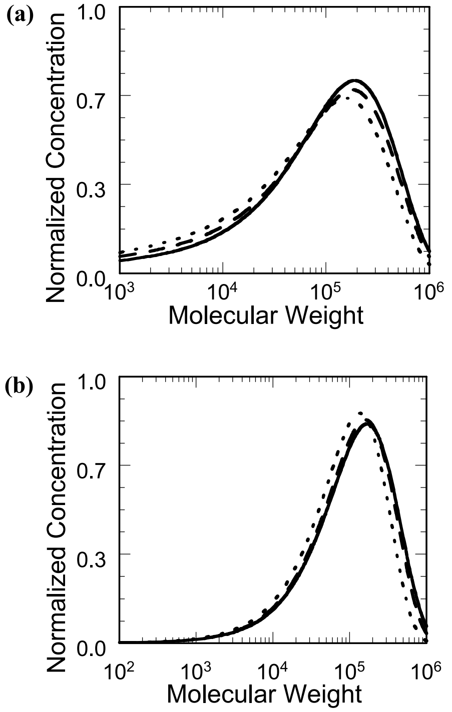

Fig. 4. MWDs are presented as determined by the model with (a) and without (b) accounting for CLDT. All photopolymerizations are simulated with 0.1 wt% DMPA at 2.5 mW/cm^2. Double bond conversions reflect values during autoacceleration (…), around the maximum polymerization rate (- - -), and during autodeceleration (—).

While chain transfer to either polymer or a unimolecular species results in very different effects on the photopolymerization kinetics, these differences are not always obvious when examining the MWD of the backbone kinetic

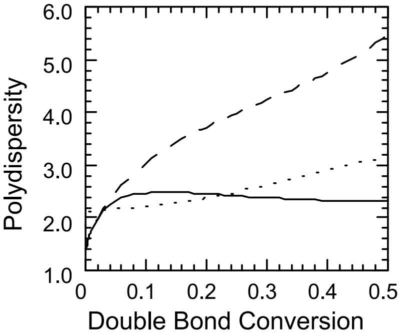

Fig. 5. The polydispersity as a function of double bond conversion is presented as determined by the CLDT model without chain transfer (—) and with chain transfer to either polymer (– – –) or a unimolecular species (…). All photopolymerizations are with 0.1 wt% DMPA at 2.5 mW/cm^2.

chains. For example, MSA's abstractable hydrogens are found between the water-labile anhydride linkages of the crosslinker spacer unit and not on the backbone kinetic chains. Therefore, upon degradation, any chain transfer to polymer to the crosslinker spacer unit will appear as chain transfer to a unimolecular species (i.e. monomer) when analyzing the degradation products. Interestingly, the effects of chain transfer to polymer on the MWD of the backbone kinetic chains during polymerization and after degradation are completely different. In contrast, diacrylate macromers based on poly(ethylene glycol) (PEG) and poly(lactic acid) (PLA) that are being developed to photopolymerize into crosslinked degradable networks for biomedical applications have very different chemistry. During photopolymerization, chain transfer to polymer would most likely occur with the tertiary hydrogen on the acrylate functionality. Thus, the MWD of the degradation products would reveal evidence of CTP to the backbone of the kinetic chains.

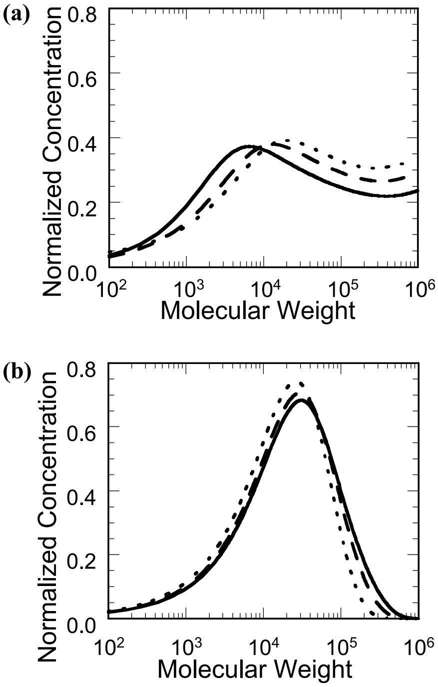

Fig. 6. MWDs are presented as determined by the CLDT model with chain transfer to either polymer (a) or a unimolecular species (b). All photopolymerizations are simulated with 0.1 wt% DMPA at 2.5 mW/cm^2. Double bond conversions reflect values during autoacceleration (…), around the maximum polymerization rate (- - -), and during autodeceleration (—).

Another way to obtain information as to the importance of kinetic chains during multivinyl monomer photopolymerization is to examine how changing the light intensity impacts network formation. Anseth and co-workers [15,17] observed that increasing the light intensity decreases the cumulative polydispersity of the final MWD of MSA's backbone kinetic chains and shifts the MWD towards a shorter average chain length. This model takes into account chain length dependencies, and thus, is ideally suited for analyzing the effect of initiation rate changes on the polymerization kinetics and structural evolution.

The impact of the light intensity on the polydispersity of the final MWD of the backbone kinetic chains was investigated when the model accounts for unimolecular termination, chain transfer to polymer, or chain transfer to a unimolecular species. The CLDT model predicts that increasing the initiation rate increases the kinetic chain length polydispersity at each double bond conversion (Fig. 7). This trend was independent of the dominant termination mechanism incorporated into the model. Additionally, all models predict that increasing the light intensity shifts the MWD towards a lower average kinetic chain length (Fig. 8).

6. Conclusions

Multivinyl monomers that react to form highly crosslinked, biodegradable networks are useful in characterizing better the complexities of the kinetics and structural evolution during crosslinking photopolymerization. A kinetic model provides insight into the fundamental mechanisms that control the MWD of the backbone kinetic chains. The unique attributes of this model, i.e. that it accounts for

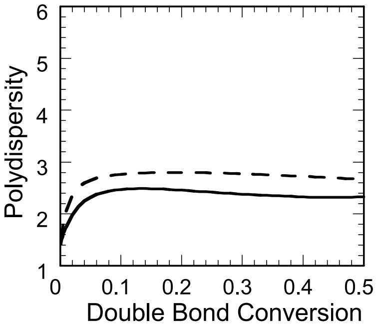

Fig. 7. The influence of the initiation rate (2.5 (—) or 25.0 (- - -) mW/cm^2 with 0.1 wt% DMPA) on the kinetic chain length polydispersity is presented as determined by the CLDT model.

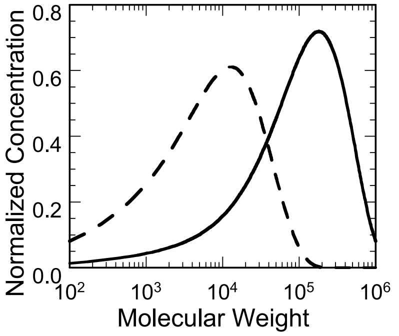

Fig. 8. The influence of the initiation rate (2.5 (—) or 25.0 (- - -) mW/cm^2 with 0.1 wt% DMPA) on the final MWD of the backbone kinetic chains is presented as determined by the CLDT model.

CLDT, chain transfer, unimolecular termination, and predicts phenomena typical of crosslinking photopolymerization, allow for systematic evaluation of the impact of the termination mechanisms and cure conditions on the shape and polydispersity of the MWD of the degradation products. Information as to how different cure conditions and monomer chemistries impact the MWD of the degradation products is important for biomaterial applications since the tails of the distribution of the polymer kinetic chains at both the very high and very low molecular weights are problematic.

Acknowledgements

The authors thank the IUCRC for Fundamentals and Applications of Photopolymerizations, and the Department of Education for granting GAANN fellowships to TML and JAB.

References

[1] Dickens SH, Stansbury JW, Choi KM, Floyd CJE. Macromolecules 2003;36(16):6043–53.
[2] Kloosterboer JG. Adv Polym Sci 1988;84:1–61.
[3] Anseth KS, Burdick JA. MRS Bull 2002;27(2):130–6.
[4] Fisher JP, Dean D, Engel PS, Mikos AG. Annu Rev Mater Res 2001;31:171–81.
[5] Decker C. Polym Int 1998;45:133–41.
[6] Anseth KS, Metters AT, Bryant SJ, Martens PJ, Elisseeff JH, Bowman CN. J Controlled Release 2002;78(1–3):199–209.
[7] Anseth KS, Newman SM, Bowman CN. Adv Polym Sci 1995;122:177–217.
[8] Decker C. Acta Polym 1994;45:333–47.
[9] Minnema L, Staverman AJ. J Polym Sci 1958;29:281–306.
[10] Dusek K. Macromolecules 1984;17:716–22.
[11] Korolev GV. Russ Chem Rev 2003;72(3):197–216.
[12] Dusek K. Makromol Chem Suppl 1979;2:35–49.
[13] Burdick JA, Peterson AJ, Anseth KS. Biomaterials 2001;22(13):1779–86.
[14] Svaldi-Muggli D, Burkoth AK, Keyser SA, Lee HR, Anseth KS. Macromolecules 1998;31(13):4120–5.
[15] Burdick JA, Lovestead TM, Anseth KS. Biomacromolecules 2003;4:149–56.
[16] Anseth KS, Shastri VR, Langer R. Nat Biotech 1999;17(2):156–9.
[17] Burkoth AK, Anseth KS. Macromolecules 1999;32(5):1438–44.
[18] Zhu S, Hamielec AE. J Polym Sci B 1994;32:929–43.
[19] Arzamendi G, Asua JM. Macromolecules 1995;28:7479–90.
[20] Tobita H, Mima T, Okada A, Mori J, Tanabe T. J Polym Sci B 1999;37:1267–75.
[21] Iedema PD, Wulkow M, Hoefsloot HCJ. Macromolecules 2000;33:7173–84.
[22] Dias RCS, Costa MRPFN. Macromolecules 2003;36:8853–63.
[23] Zhu S. Macromolecules 1996;29:456–61.
[24] Fiorentino S, Ghielmi A, Storti G, Morbidelli M. Ind Eng Chem Res 1997;36:1283–301.
[25] Tobita H. Macromol Theory Simul 1998;7:225–32.
[26] Nikitin A, Castignolles P, Charleux B, Vairon J-P. Macromol Theory Simul 2003;12:440–8.
[27] Nikitin A, Evseev AV, Buback M, Feldermann A, Jurgens M, Nelke D. Macromol Theory Simul 2002;11((961–968)).
[28] Yu Q, Nauman S, Santerre JP, Zhu S. J Mater Sci 2001;36:3599–605.
[29] O'Neil GA, Torkelson JM. Macromolecules 1999;32:411–22.
[30] O'Neil GA, Wisnudel MB, Torkelson JM. Macromolecules 1998;31:4537–45.
[31] Ivanov VA, Kaninskii VA, Brun YB, Korolev BA, Lachinov MB. Polym Sci 1991;33(7):1336–47.
[32] Cardenas JN, O'Driscoll KF. Polym Chem Ed 1976;14:883–97.
[33] Chiu WY, Carratt GM, Soong DS. Macromolecules 1983;16(3):348–57.
[34] Achilias DS, Kiparissides C. Macromolecules 1992;25:3739–50.
[35] Soh SK, Sundberg DC. J Polym Sci, Polym Chem Ed 1982;20:1299–313.
[36] Tulig TJ, Tirrell M. Macromolecules 1981;14:1501–11.
[37] Berchtold KA, Lovestead TM, Bowman CN. Macromolecules 2002;35:7968–75.
[38] Young JS, Bowman CN. Macromolecules 1999;32:6073–81.
[39] Russell GT, Napper DH, Gilbert RG. Macromolecules 1988;21:2133–40.
[40] Anseth KS, Wang CM, Bowman CN. Macromolecules 1994;27(3):650–5.
[41] Buback M, Huckestein B, Russell GT. Macromol Chem Phys 1994;195(2):539–54.
[42] Soh SK, Sundberg DC. J Polym Sci, Polym Chem Ed 1982;20:1315–29.
[43] Marten FL, Hamielec AE. J Appl Polym Sci 1982;27:489–505.
[44] Allen PEM, Patrick CR. Makromol Chem 1961;47:154–67.
[45] Soh SK, Sundberg DC. J Polym Sci, Polym Chem Ed 1982;20:1331–44.
[46] Batch GL, Macosko CW. J Appl Polym Sci 1992;44:1711–29.
[47] O'Neil GA, Wisnudel MB, Torkelson JM. AIChE J 1998;44(5):1226–31.
[48] Odian G. Principles of polymerization. 3rd ed. New York: Wiley; 1991.
[49] Flory PJ. Principles of polymer chemistry. 1st ed. Ithaca: Cornell University Press; 1953.
[50] Benson SW, North AM. J Am Chem Soc 1962;84:935–40.
[51] Buback M, Egorov M, Gilbert RG, Kaminsky V, Olaj OF, Russell GT, et al. Macromol Chem Phys 2002;203:2570–82.
[52] de Kock JBL, Van Herk AM, German AL. J Macromol Sci Polym Rev 2001;3:199–252.
[53] Kamachi M. Makromol Chem Suppl 1985;14:17–27.
[54] Mahabadi H. Macromolecules 1991;24:606–9.
[55] Olaj OF, Kornherr A, Vana P, Zoder M, Zifferer G. Macromol Symp 2002;182:15–30.
[56] Russell G. Aust J Chem 2002;55:399–414.
[57] Russell GT, Gilbert RG, Napper DH. Macromolecules 1992;25(9):2459–69.
[58] Russell GT. Macromol Theory Simul 1995;4(3):519–48.

[59] Berchtold KA, Lovell LG, Nie J, Hacioglu B, Bowman CN. Polymer 2001;42:4925–9.

[60] Berchtold KA, Hacioglu B, Lovell L, Nie J, Bowman CN. Macromolecules 2001;34:5103–11.

[61] Lovestead TM, Berchtold KA, Bowman CN. Macromol Theory Simul 2002;11:729–38.

[62] Goodner MD, Bowman CN. Chem Eng Sci 2002;57:887–900.

[63] Goodner MD, Lee HR, Bowman CN. Ind Eng Chem Res 1997;36(4): 1247–52.

[64] Anseth KS, Bowman CN. Polym React Eng 1993;1(4):4999–520.

[65] Bowman CN, Peppas NA. Macromolecules 1991;24(8):1914–20.

[66] Lovestead TM, O'Brien AK, Bowman CN. J Photoch Photobio A 2003;159(2):135–43.

[67] Bueche F. Physical properties of polymers. London: Interscience; 1962.

[68] Wen M, McCormick AV. Macromolecules 2000;33:9247–54.

[69] Kannurpatti AR, Anderson KJ, Anseth JW, Bowman CN. J Polym Sci, Part B: Polym Phys 1997;35(14):2297–307.

[70] Anseth KS, Kline LM, Walker TA, Anderson KJ, Bowman CN. Macromolecules 1995;28:2491–9.

[71] Busfield WK. Heats and entropies of polymerization, ceiling temperatures, equilibrium monomer concentrations; and polymerizability of heterocyclic compounds. In: Brandrup J, Immergut EH, editors. Polymer handbook. New York: Wiley; 1989. p. II/295.